

ENERGY INJECTION FOR MECHANICAL SYSTEMS THROUGH THE METHOD  
OF VIRTUAL NONHOLONOMIC CONSTRAINTS

by

Adan Moran-MacDonald

A thesis submitted in conformity with the requirements  
for the degree of Master of Applied Science  
Graduate Department of Electrical and Computer Engineering  
University of Toronto

© Copyright 2020 by Adan Moran-MacDonald

# **Abstract**

Energy injection for mechanical systems through the method of Virtual Nonholonomic Constraints

Adan Moran-MacDonald

Master of Applied Science

Graduate Department of Electrical and Computer Engineering

University of Toronto

2020

**TODO:** Fill in the abstract

For Fry.

# Acknowledgements

**TODO:** Fill in the acknowledgements

# Contents

<b>List of Symbols</b>	<b>vii</b>
<b>1 Introduction</b>	<b>2</b>
1.1 Literature Review . . . . .	2
1.2 Statement of Contributions . . . . .	2
1.3 Outline of the Thesis . . . . .	2
<b>2 Development of Virtual Nonholonomic Constraints</b>	<b>3</b>
2.1 Preliminaries on Analytical Mechanics . . . . .	3
2.1.1 Lagrangian Mechanics . . . . .	5
2.1.2 Hamiltonian Mechanics . . . . .	6
2.2 Simply Actuated Hamiltonian Systems . . . . .	7
2.3 Virtual Nonholonomic Constraints . . . . .	10
2.4 Summary of Results . . . . .	17
<b>3 Application of VNHCS: The Variable Length Pendulum</b>	<b>18</b>
3.1 Motivation . . . . .	18
3.2 Dynamics of the Variable Length Pendulum . . . . .	18
3.3 The VLP Constraint . . . . .	21
3.4 Simulation Results . . . . .	27
<b>4 Application of VNHCS: The Acrobot</b>	<b>28</b>
4.1 Motivation . . . . .	28
4.2 Dynamics of the Acrobot . . . . .	29
4.3 Previous Approaches . . . . .	30
4.4 The Acrobot Constraint . . . . .	30
4.5 Proving the Acrobot Gains Energy . . . . .	30
4.6 Experimental Results . . . . .	30

<b>5 Conclusion</b>	<b>31</b>
5.1 Limitations of this Work . . . . .	31
5.2 Future Research . . . . .	31
<b>Bibliography</b>	<b>31</b>

# List of Symbols

Symbol	Definition
$\mathbf{n}$	The index set $\{1, \dots, n\}$ of natural numbers up to $n$ .
$\mathbb{R}^n$	Real numbers in $n$ dimensions.
$[\mathbb{R}]_T$	Real numbers modulo $T > 0$ , with $[\mathbb{R}]_\infty = \mathbb{R}$ .
$\mathbb{S}^1$	The unit circle, equivalent to $[\mathbb{R}]_{2\pi}$ .
$\mathcal{Q}$	The configuration manifold of a system.
$\mathbb{R}^{n \times m}$	The space of real-valued matrices with $n$ rows and $m$ columns.
$I_n$	The $n \times n$ identity matrix.
$\mathbf{0}_{n \times m}$	The $n \times m$ matrix of all zeros.
$M_i$	If $M$ is a vector, the $i$ th element of $M$ . If $M$ is a matrix, the $i$ th column of $M$ .
$M_{i,j}$	The value of row $i$ , column $j$ for the matrix $M$ .
$\dot{x}$	Derivative of $x$ with respect to time $t$ .
$\nabla_v F$	If $F$ is $\mathbb{R}$ -valued, the gradient of $F$ with respect to $v$ . If $F : \mathbb{R}^m \rightarrow \mathbb{R}^{n \times n}$ , the block matrix gradient $(\frac{\partial F}{\partial v_1}, \dots, \frac{\partial F}{\partial v_m}) \in \mathbb{R}^{nm \times n}$ .
$dF_v$	Total differential (Jacobian) of $F$ , equivalent to $(\nabla_v F)^\top$ .
$\text{Hess } F$	If $F : \mathbb{R}^n \rightarrow \mathbb{R}$ , the $n \times n$ Hessian matrix of double derivatives of $F$ . If $F : \mathbb{R}^n \rightarrow \mathbb{R}^k$ , the block matrix $(\text{Hess } F_1, \dots, \text{Hess } F_k) \in \mathbb{R}^{n \times nk}$ .
$\partial_v \partial_w F$	Derivative matrix of $F : \mathbb{R}^n \times \mathbb{R}^m \rightarrow \mathbb{R}$ , with $(i, j)$ element $\frac{\partial^2 F}{\partial v_i \partial w_j}$ .
$\delta_{i,j}$	The Kronecker delta: 1 if $i = j$ and 0 otherwise.
$\otimes$	The matrix kronecker product (see Appendix ???).

## TEST CITATIONS:

[1] [2] [3] [4] [5] [6] [7] [8] [9] [10] [11] [12] [13] [14] [15] [16] [17] [18] [19] [20] [21]  
[22] [23] [24] [25] [26] [27] [28] [29] [30] [31] [32] [33] [34] [35] [36] [37] [38] [39] [40]  
[41] [42] [43] [44] [45] [46] [47] [48] [49]



# **Chapter 1**

## **Introduction**

### **1.1 Literature Review**

### **1.2 Statement of Contributions**

### **1.3 Outline of the Thesis**

## Chapter 2

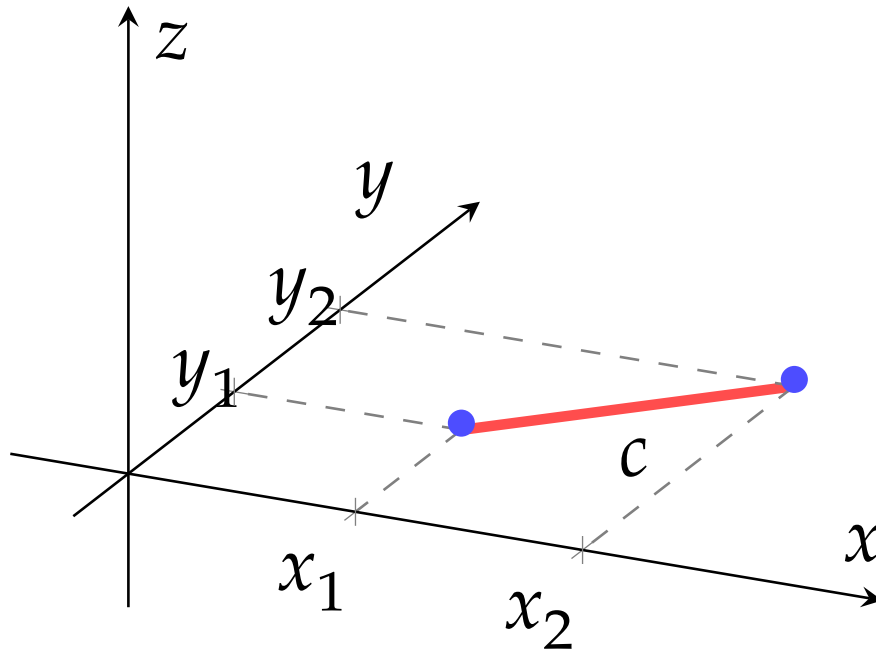
# Development of Virtual Nonholonomic Constraints

### 2.1 Preliminaries on Analytical Mechanics

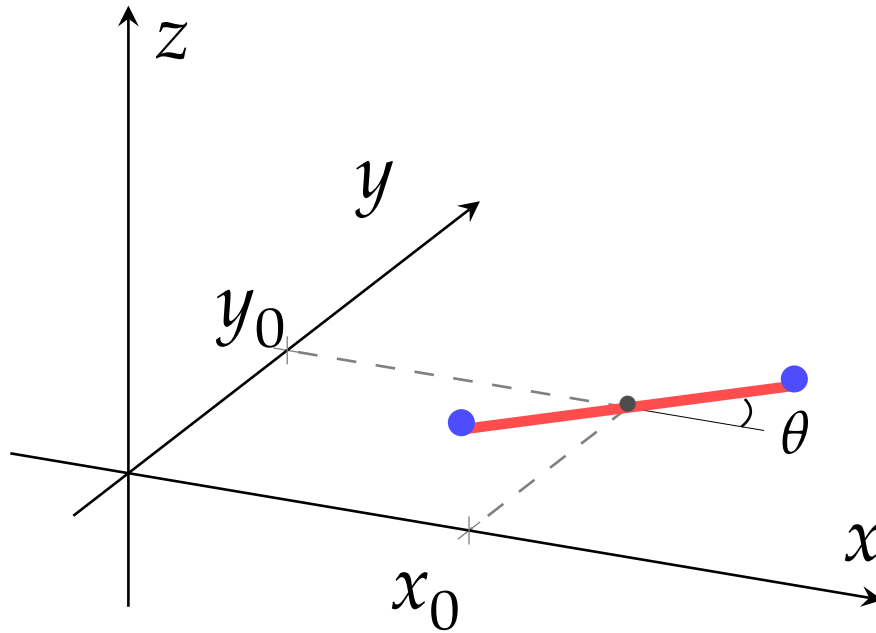
A mechanical system can be represented by  $N$  point masses where each point represents the center of mass of a physical body, along with  $r$  *equations of constraint* (EOC) which model the physical restrictions between these masses. The position of each point mass is described using three cartesian coordinates (one for each spatial axis), so the system as a whole can be described by a vector in  $\mathbb{R}^{3N}$  with  $r$  EOC. The dynamics of the system are computed by deriving the  $3N$  *equations of motion* (EOM) produced by Newton's second law  $F = ma$ . While this technique works for simple systems, it is tedious and becomes impossible to apply to complex mechanical systems where the forces are not explicitly known.

Rather than modeling a mechanical system by cartesian positions and constraints, it is often feasible to represent the position of the system using  $n$  independent scalar-valued variables  $q_1, \dots, q_n$  called *generalized coordinates*, where  $n = 3N - r$  is the number of *degrees of freedom* (DOF) of the system [23]. For instance, Figure 2.1 shows a barbell on a 2D-plane which can rotate freely on that plane. The barbell has  $n = 3$  DOF, so it can be described by three independent generalized coordinates with no equations of constraint.

For the robotic systems of interest in this thesis, we assume that each generalized coordinate  $q_i$  represents either the distance or the angle between two parts of the system. Mathematically, each  $q_i$  takes values in  $[\mathbb{R}]_{T_i}$ , where  $T_i = \infty$  if  $q_i$  represents a length or  $T_i = 2\pi$  if  $q_i$  represents an angle. It is convention to collect the coordinates into a



(A) The Newtonian representation of the barbell requires all six cartesian positions and the corresponding EOC.



(B) One possible set of three generalized coordinates is  $(x_0, y_0, \theta)$ , which represent the position of the center of the bar and the angle of the barbell in the  $xy$ -plane.

FIGURE 2.1: A mechanical system with  $N = 2$  points at  $(x_1, y_1, z_1)$  and  $(x_2, y_2, z_2)$  separated by a bar with  $r = 3$  EOC given by  $c = \|x_1 - x_2\|$ ,  $z_1 = 0$ , and  $z_2 = 0$ . This system has  $n = 3$  degrees of freedom.

configuration  $q = (q_1, \dots, q_n) \in \mathcal{Q}$  where the *configuration manifold*  $\mathcal{Q}$  of the system is a so-called *generalized cylinder*:

$$\mathcal{Q} = [\mathbb{R}]_{T_1} \times \dots \times [\mathbb{R}]_{T_n}$$

The derivative  $\dot{q} = (\dot{q}_1, \dots, \dot{q}_n)$  of a configuration is called a *generalized velocity* of the system. For arbitrary systems, the space of allowable velocities depends on the current configuration of the system. However, since  $\mathcal{Q}$  is a generalized cylinder, we find that  $\dot{q} \in \mathbb{R}^n$ . The combined vector  $(q, \dot{q}) \in \mathcal{Q} \times \mathbb{R}^n$  is called a *state* of the system.

The field of analytical mechanics provides a computational method for finding the EOM of a system in generalized coordinates. The two most common analytical methods for modelling robotic systems are *Lagrangian* and *Hamiltonian* mechanics.

### 2.1.1 Lagrangian Mechanics

Lagrangian mechanics uses the kinetic energy  $T(q, \dot{q})$  and potential energy  $P(q)$  of the system to define the Lagrangian  $\mathcal{L} : \mathcal{Q} \times \mathbb{R}^n \rightarrow \mathbb{R}$  defined by (2.1) [23].

$$\mathcal{L}(q, \dot{q}) = T(q, \dot{q}) - P(q) \quad (2.1)$$

When the mechanical system is actuated, the EOM are described by  $n$  second-order ordinary differential equations (ODEs) obtained from the *Euler-Lagrange equations* (2.2) with *generalized input forces*  $\tau \in \mathbb{R}^k$ .

$$\frac{d}{dt} \left\{ \frac{\partial \mathcal{L}}{\partial \dot{q}_i} \right\} - \frac{\partial \mathcal{L}}{\partial q_i} = B_i^\top(q) \tau \quad (2.2)$$

The vector  $B_i^\top : \mathcal{Q} \rightarrow \mathbb{R}^{1 \times k}$  describes how the input forces shape the dynamics of  $q_i$ . The matrix  $B : \mathcal{Q} \rightarrow \mathbb{R}^{n \times k}$  with

$$B(q) = \begin{bmatrix} - & B_1^\top(q) & - \\ & \vdots & \\ - & B_n^\top(q) & - \end{bmatrix}$$

is called the *input matrix* for the system. If  $k < n$ , we say the system is *underactuated* with degree of underactuation  $(n - k)$ .

Many actuated mechanical systems have quadratic kinetic energies, so that the Lagrangian can be written explicitly as

$$\mathcal{L}(q, \dot{q}) = \frac{1}{2} \dot{q}^\top D(q) \dot{q} - P(q) \quad (2.3)$$

where the *inertia matrix*  $D : \mathcal{Q} \rightarrow \mathbb{R}^{n \times n}$  is a symmetric, positive definite matrix for all  $q \in \mathcal{Q}$  and the potential function  $P : \mathcal{Q} \rightarrow \mathbb{R}$  is smooth.

### 2.1.2 Hamiltonian Mechanics

Hamiltonian mechanics converts the  $n$  second-order ODEs generated by Lagrangian mechanics into an equivalent set of  $2n$  first-order ODEs.

To do this, we first define the *conjugate of momentum*  $p_i$  to  $q_i$  by

$$p_i(q, \dot{q}) := \frac{\partial \mathcal{L}}{\partial \dot{q}_i}(q, \dot{q}) \quad (2.4)$$

To ease notation, we write  $p = (p_1, \dots, p_n) \in \mathbb{R}^n$  and call  $p$  the *conjugate of momenta* to  $q$ . Note that each  $p_i$  is a linear function of  $\dot{q}$ , and one can typically solve for  $\dot{q}(q, p)$  by inverting all the expressions from (2.4). The combined vector  $(q, p) \in \mathcal{Q} \times \mathbb{R}^n$  is called a *phase* of the system.

The *Hamiltonian* of the system in  $\{q, p\}$  coordinates is the “Legendre transform” (2.5) of the Lagrangian [24].

$$\mathcal{H}(q, p) := p^\top \dot{q}(q, p) - \mathcal{L}(q, \dot{q}(q, p)) \quad (2.5)$$

The EOM in the Hamiltonian framework are the  $2n$  first-order equations called *Hamilton’s equations*. They are given by:

$$\begin{cases} \dot{q} = \nabla_p \mathcal{H} \\ \dot{p} = -\nabla_q \mathcal{H} + B(q)\tau \end{cases} \quad (2.6)$$

Here,  $B(q) \in \mathbb{R}^{n \times k}$  is the same input matrix used by the Lagrangian framework, with  $\tau \in \mathbb{R}^k$  the same vector of generalized input forces.

If the kinetic energy of the system is quadratic as in (2.3), the conjugate of momenta becomes  $p = D(q)\dot{q}$ . Since  $D(q)$  is symmetric and positive definite, it is invertible at each  $q \in \mathcal{Q}$ . The resulting Hamiltonian system reduces to (2.7).

$$\mathcal{H}(q, p) = \frac{1}{2} p^\top D^{-1}(q) p + P(q) \quad (2.7)$$

$$\begin{cases} \dot{q} = D^{-1}(q) p \\ \dot{p} = -\frac{1}{2} (I_n \otimes p^\top) \nabla_q D^{-1}(q) p - \nabla_q P(q) + B(q)\tau \end{cases} \quad (2.8)$$

Any set of coordinates  $\{q, p\}$  which satisfy Hamilton's equations under the Hamiltonian  $\mathcal{H}$  are said to be *canonical coordinates* for the system. A change of coordinates  $(q, p) \rightarrow (Q, P)$  is a *canonical transformation* if  $\{Q, P\}$  preserve the Hamiltonian structure; that is, if they are canonical coordinates under the Hamiltonian  $\mathcal{H}(q(Q, P), p(Q, P))$ .

## 2.2 Simply Actuated Hamiltonian Systems

**Manfredi:** What term should we use instead of “simply actuated”?

Suppose we are given a Hamiltonian mechanical system (2.7). Because  $\tau$  is transformed by the input matrix  $B(q)$  before entering the EOM, it is not in general clear how any particular input force  $\tau_i$  will affect the dynamics of the system. In this section, we define a new class of Hamiltonian systems where the effect of the input forces is made obvious. This class of systems will form the backbone for the rest of the theory developed in this thesis.

**Definition 1.** Let  $\mathcal{H}$  be an  $n$ -DOF Hamiltonian system with  $k \leq n$  actuators. A set of canonical coordinates  $\{q, p\}$  for this system are said to be *simply actuated coordinates* if the input matrix  $B(q) \in \mathbb{R}^{n \times k}$  is of the form

$$B(q) = \begin{bmatrix} \mathbf{0}_{(n-k) \times k} \\ I_k \end{bmatrix}$$

The first  $(n - k)$  coordinates, labelled  $q_u$ , are called the *unactuated coordinates*. The remaining  $k$  coordinates, labelled  $q_a$ , are called the *actuated coordinates*. When grouping them together, we will always put them in the order  $(q_u, q_a)$  to fit with the definition. The corresponding  $(p_u, p_a)$  are called the unactuated and actuated momenta, respectively.

**Definition 2.** A Hamiltonian system is said to be *simply actuated* if there exists a canonical transformation from any canonical coordinates  $\{q, p\}$  into simply actuated coordinates.

Under the following assumptions on the input matrix, we will show that the Hamiltonian system (2.7) is simply actuated.

**Assumption 1.** The input matrix  $B(q) \equiv B \in \mathbb{R}^{n \times k}$  is constant, full rank, and  $k < n$ .

**Assumption 2.** There exists a matrix  $B^\perp \in \mathbb{R}^{(n-k) \times n}$  which is right semi-orthogonal ( $B^\perp (B^\perp)^\top = I_{(n-k)}$ ) and which is a left-annihilator for  $B$ . That is,  $B^\perp B = \mathbf{0}_{(n-k) \times k}$ .

Note that if  $k = (n - 1)$ , the existence of any left annihilator  $A^0 \in \mathbb{R}^{1 \times n}$  implies the left annihilator  $B^\perp := A^0 / \|A^0\|$  satisfies Assumption 2.

**Assumption 3.** Assume **without loss of generality** that the input matrix  $B$  is left semi-orthogonal. That is,  $B^\top B = I_k$ .

*Proof.* Since  $B$  is a constant matrix, it has a singular-value decomposition  $B = U\Sigma V^\top$  where  $U^{-1} = U^\top \in \mathbb{R}^{n \times n}$ ,  $V^{-1} = V^\top \in \mathbb{R}^{k \times k}$ , and  $\Sigma \in \mathbb{R}^{n \times k}$  is defined by

$$\Sigma = \begin{bmatrix} \sigma_1 & 0 & \cdots & 0 \\ 0 & \sigma_2 & \cdots & 0 \\ \vdots & & \ddots & \vdots \\ 0 & 0 & \cdots & \sigma_k \\ - & \mathbf{0}_{(n-k) \times k} & - & - \end{bmatrix}$$

where  $\sigma_i \neq 0$  because  $B$  is full-rank [49]. Defining  $T \in \mathbb{R}^{k \times k}$  by

$$T = \begin{bmatrix} \frac{1}{\sigma_1} & 0 & \cdots & 0 \\ 0 & \frac{1}{\sigma_2} & \cdots & 0 \\ \vdots & & \ddots & \vdots \\ 0 & 0 & \cdots & \frac{1}{\sigma_k} \end{bmatrix}$$

and assigning the input forces to  $\tau = VT\hat{\tau}$ , we get a new input matrix for  $\hat{\tau} \in \mathbb{R}^k$  given by  $\hat{B} = BVT = U\Sigma T$  which is still constant and full-rank. In particular,  $\hat{B}^\top \hat{B} = T^\top \Sigma^\top \Sigma T = I_k$ .  $\square$

Let  $\mathbf{B} \in \mathbb{R}^{n \times n}$  be the following matrix:

$$\mathbf{B} = \begin{bmatrix} B^\perp \\ B^\top \end{bmatrix}$$

Since  $B^\perp$  is a left annihilator of  $B$  and both  $B^\perp$  and  $B^\top$  are right semi-orthogonal, it is easy to show that  $\mathbf{B}$  is orthogonal:

$$\mathbf{B}\mathbf{B}^\top = \begin{bmatrix} B^\perp (B^\perp)^\top & B^\perp B^\top \\ (B^\perp B)^\top & B^\top B \end{bmatrix} = I_n$$

Hence,  $\mathbf{B}$  is invertible with  $\mathbf{B}^{-1} = \mathbf{B}^\top$ .

The following theorem shows that  $\mathbf{B}$  provides a canonical transformation into simply actuated coordinates, so that only the actuated momenta are affected by the input forces.

**Theorem 1.** *Under Assumptions 1,2, and 3, the Hamiltonian system (2.7) is simply actuated with simply actuated coordinates  $\{Q = \mathbf{B}q, P = \mathbf{B}p\}$ . The resulting dynamics are given by (2.9),*

$$\begin{aligned} \mathcal{H}(Q, P) &= \frac{1}{2} P^\top M^{-1}(Q) P + V(Q) \\ \begin{cases} \dot{Q} = M^{-1}(Q) P \\ \dot{P} = -\frac{1}{2} (I_n \otimes P^\top) \nabla_Q M^{-1}(Q) P - \nabla_Q V(Q) + \begin{bmatrix} \mathbf{0}_{(n-k) \times k} \\ I_k \end{bmatrix} \tau \end{cases} \end{aligned} \quad (2.9)$$

where

$$\begin{aligned} M^{-1}(Q) &:= \mathbf{B} D^{-1} (\mathbf{B}^\top Q) \mathbf{B}^\top \\ V(Q) &:= P (\mathbf{B}^\top Q) \end{aligned}$$

*Proof.* The Poisson bracket between the functions  $f(q, p)$  and  $g(q, p)$  is defined by [24] as follows:

$$[f, g] := \sum_{i=1}^n \frac{\partial f}{\partial p_i} \frac{\partial g}{\partial q_i} - \frac{\partial f}{\partial q_i} \frac{\partial g}{\partial p_i}$$

For any constant matrix  $A$ , the transformation  $\{Q = Aq, P = Ap\}$  satisfies  $\frac{\partial Q_i}{\partial p_m} = \frac{\partial P_i}{\partial q_m} = 0$  for all  $i, m \in \mathbf{n}$ . Hence, for our new coordinates  $\{Q = \mathbf{B}q, P = \mathbf{B}p\}$ ,

$$\begin{aligned} [Q_i, Q_j] &:= \sum_{m=1}^n \frac{\partial Q_i}{\partial p_m} \frac{\partial Q_j}{\partial q_m} - \frac{\partial Q_i}{\partial q_m} \frac{\partial Q_j}{\partial p_m} = 0 \\ [P_i, P_j] &:= \sum_{m=1}^n \frac{\partial P_i}{\partial p_m} \frac{\partial P_j}{\partial q_m} - \frac{\partial P_i}{\partial q_m} \frac{\partial P_j}{\partial p_m} = 0 \end{aligned}$$

Since the matrix  $\mathbf{B}$  is orthogonal,  $(\mathbf{B}_i)^\top (\mathbf{B}^\top)_j = (\mathbf{B}_i)^\top (\mathbf{B}^{-1})_j = \delta_{i,j}$ . Using this fact we see that the Poisson brackets between  $P_i$  and  $Q_j$  are given by:

$$\begin{aligned} [P_i, Q_j] &= \sum_{m=1}^n \frac{\partial P_i}{\partial p_m} \frac{\partial Q_j}{\partial q_m} - \frac{\partial P_i}{\partial q_m} \frac{\partial Q_j}{\partial p_m} \\ &= \sum_{m=1}^n \mathbf{B}_{i,m} \mathbf{B}_{j,m} - 0 \\ &= \sum_{m=1}^n \mathbf{B}_{i,m} \mathbf{B}_{m,j}^\top \\ &= (\mathbf{B}_i)^\top \mathbf{B}_j^\top \\ &= \delta_{i,j} \end{aligned}$$



Therefore, by (45.10) in [24], the coordinate change  $(Q = Bq, P = Bp)$  is a canonical transformation. Furthermore, since  $\dot{P} = B\dot{p}$ , the new input matrix is given by

$$BB = \begin{bmatrix} B^\perp B \\ B^\top B \end{bmatrix} = \begin{bmatrix} 0_{(n-k) \times k} \\ I_k \end{bmatrix}$$

so the coordinates  $\{Q = (q_u, q_a), P = (p_u, p_a)\}$  are simply actuated coordinates for  $\mathcal{H}$  as desired.  $\square$

## 2.3 Virtual Nonholonomic Constraints

Let us imagine a child on a swing who wants to reach the largest height possible. To begin, the child pushes off the ground to imbue the swing with small oscillations. What allows them to increase the amplitude of these oscillations is the appropriate extension and retraction of their feet. If a roboticist were creating a machine to replicate this behaviour, they might design a robot whose legs extend and retract at specific time intervals. At first glance, this technique should work perfectly because the leg motion would synchronize with the swinging frequency, thereby injecting energy as quickly as is physically possible.

Unfortunately, a deeper analysis reveals the flaw with this design. Most children are not counting out the time in their head; rather, they observe their current position and velocity and adjust their legs as required. For example, many children have an adult pushing the swing, or perhaps they are swinging on a windy day. In either case, they adjust their leg motion accordingly when presented with these external disturbances, without keeping track of time. Hence, the standard control technique of tracking a function of time (known as *trajectory tracking*) does not truly replicate human behaviour. Even if the robot's legs perfectly track a specified trajectory, an external disturbance will desynchronize the leg motion with the swing - thereby stopping the amplitude-increasing effects.

Rather than tracking a trajectory over time, a more human-like behaviour is to force the robot's legs track a function of the swing's state. One recent control method known as *virtual holonomic constraints* (VHCs) uses the actuators to enforce a relation  $h(q) = 0$  of the configuration [19]. This method has provided incredible results in the development of walking robots [27, 28], vehicle motion [30, 31], and has even been used to design a snake-like swimming robot [29].

The downside to VHCs is that they do not use the additional information imparted

by the velocity of a system. For the child on a swing, whether they extend or retract their legs depends on their direction of motion. This inherently requires knowledge of their current velocity, which precludes the usage of VHCs. Many authors have attempted to extend the theory of VHCs to enforce relations  $h(q, \dot{q}) = 0$  of the full state to account for this drawback. Since these relations use actuators to restrict both the configuration and velocity of a system, they are called virtual *nonholonomic* constraints. This idea has been used for human-robot interaction [32–34], error-reduction on time-delayed systems [35], and has shown marked improvements to the field of bipedal locomotion [9, 36, 38]. Most interestingly, this nonholonomic approach is more robust than standard VHCs when applied to bipedal robotics [37]. In particular, virtual nonholonomic constraints may be capable of injecting and dissipating energy from a system in a robust manner, all while producing realistic biological motion. This is what we aim to prove in this thesis.

Unlike the theory of VHCs, there does not appear to be a standard definition of virtual nonholonomic constraints: all the applications listed above use their own definitions, which makes it difficult to compare and generalize their work.

This section will provide a standard characterization of virtual nonholonomic constraints using Hamiltonian mechanics. The goal is to provide a consistent, rigorous foundation for designing constraints on a general class of systems.

**Definition 3.** A *virtual nonholonomic constraint* (VNHC) of order  $k$  is a relation  $h(q, p) = 0$  where  $h : \mathcal{Q} \times \mathbb{R}^n \rightarrow \mathbb{R}^k$  is smooth,  $\text{rank}([dh_q, dh_p]) = k$  for all  $(q, p) \in h^{-1}(0)$ , and there exists a feedback controller  $\tau(q, p)$  stabilizing the set

$$\Gamma = \{(q, p) \mid h(q, p) = 0, dh_q \dot{q} + dh_p \dot{p} = 0\}$$

which is called the *constraint manifold*.

If we define the error term  $e = h(q, p)$ , stabilizing  $\Gamma$  is equivalent to solving for the controller  $\tau(q, p)$  which drives  $e \rightarrow 0$  and  $\dot{e} \rightarrow 0$ . Supposing there is no further structure on the VNHC, then  $\dot{e} = dh_q \dot{q} + dh_p \dot{p}$ . Since  $B(q)\tau$  appears inside  $\dot{p}$ , solving for  $\tau$  explicitly requires  $dh_p(q, p)B(q) \in \mathbb{R}^{k \times k}$  to be invertible for all  $(q, p)$ .

This condition severely restricts the types of constraints one can use. It is preferable instead to have the torque  $\tau$  appear after two derivatives of  $e$  to allow for more freedom in choosing a constraint. Mathematically, if each  $\tau_i$  appears only after two derivatives, one says that  $e$  is of *relative degree*  $\{2, 2, \dots, 2\}$ . We thus define a special type of VNHC which satisfies this property.

**Definition 4.** A VNHC  $h(q, p) = 0$  of order  $k$  is *regular* if the output  $e = h(q, p)$  is of relative degree  $\{2, 2, \dots, 2\}$  everywhere on the constraint manifold  $\Gamma$ .

The authors of [9, 36, 37] observed that a relation which uses only the unactuated conjugate of momentum cannot have  $\tau$  appearing after only one derivative. Of course, they performed their research in Lagrangian form; for us to be able to use the Hamiltonian coordinate  $p_u$ , we must continue with the following assumption for the rest of the chapter.

**Assumption 4.** The mechanical system under consideration is a Hamiltonian system with  $n$  degrees of freedom and  $k < n$  actuators. It is described in simply actuated coordinates  $\{q = (q_u, q_a), p = (p_u, p_a)\}$  and has the following dynamics:

$$\begin{aligned} \mathcal{H}(q, p) &= p^\top M^{-1}(q)p + V(q) \\ \begin{cases} \dot{q} = M^{-1}p \\ \dot{p} = -\frac{1}{2}(I_n \otimes p^\top) \nabla_q M^{-1}(q)p - \nabla_q V(q) + \begin{bmatrix} \mathbf{0}_{(n-k) \times k} \\ I_k \end{bmatrix} \tau \end{cases} \end{aligned}$$

*Notation 1.* We will write  $q_u \in \mathcal{Q}_u$ ,  $q_a \in \mathcal{Q}_a$  where  $\mathcal{Q}_u \times \mathcal{Q}_a = \mathcal{Q}$ . We also write  $p_u \in \mathcal{P}_u := \mathbb{R}^{n-k}$  and  $p_a \in \mathcal{P}_a := \mathbb{R}^k$ , so that  $p \in \mathcal{P} := \mathcal{P}_u \times \mathcal{P}_a = \mathbb{R}^n$ . In this manner, the phase space of our system can be written as  $\mathcal{Q} \times \mathcal{P}$ .

**Theorem 2.** A VNHC  $h(q, p) = 0$  of order  $k$  is regular if and only if  $dh_{p_a} = 0$  and

$$\text{rank} \left( \left( dh_q M^{-1}(q) - dh_{p_u} (I_{n-k} \otimes p^\top) \nabla_{q_u} M^{-1}(q) \right) \begin{bmatrix} \mathbf{0}_{(n-k) \times k} \\ I_k \end{bmatrix} \right) = k$$

everywhere on the constraint manifold  $\Gamma$ . That is, a regular VNHC is a function  $h : \mathcal{Q} \times \mathcal{P}_u \rightarrow \mathbb{R}^k$  which satisfies the rank condition.

*Proof.* Let  $e = h(q, p) \in \mathbb{R}^k$ . Then

$$\begin{aligned} \dot{e} &= dh_q \dot{q} + dh_p \dot{p} \\ &= dh_q M^{-1}(q)p + \\ &\quad \begin{bmatrix} dh_{p_u} & dh_{p_a} \end{bmatrix} \left( -\frac{1}{2} \begin{bmatrix} (I_{n-k} \otimes p^\top) \nabla_{q_u} M^{-1}(q)p \\ (I_k \otimes p^\top) \nabla_{q_a} M^{-1}(q)p \end{bmatrix} - \begin{bmatrix} \nabla_{q_u} V(q) \\ \nabla_{q_a} V(q) \end{bmatrix} + \begin{bmatrix} \mathbf{0}_{(n-k) \times k} \\ I_k \end{bmatrix} \tau \right) \end{aligned}$$

If  $dh_{p_a} \neq \mathbf{0}_{k \times k}$  for some  $(q, p)$  on  $\Gamma$ , then  $\tau$  appears in  $\dot{e}$  and the VNHC is not of relative degree  $\{2, 2, \dots, 2\}$ . Hence, we must have that  $dh_{p_a} = \mathbf{0}_{k \times k}$ . Proceeding with this

assumption, we now find that  $h : \mathcal{Q} \times \mathcal{P}_u \rightarrow \mathbb{R}^k$ , which means that

$$\dot{e} = dh_q M^{-1}(q)p - dh_{p_u} \left( \frac{1}{2} (I_{n-k} \otimes p^\top) \nabla_{q_u} M^{-1}(q)p + \nabla_{q_u} V(q) \right)$$

Taking one further derivative provides

$$\begin{aligned} \ddot{e} = & \frac{d}{dt} \{dh_q\} M^{-1}(q)p + dh_q \left( \sum_{i=1}^n \frac{\partial M^{-1}}{\partial q_i}(q) \dot{q}_i \right) p + dh_q M^{-1}(q) \dot{p} - \\ & \frac{d}{dt} \{dh_{p_u}\} \left( \frac{1}{2} (I_{n-k} \otimes p^\top) \nabla_{q_u} M^{-1}(q)p + \nabla_{q_u} V(q) \right) - \\ & dh_{p_u} \left( \frac{1}{2} \frac{d}{dt} \{ (I_{n-k} \otimes p^\top) \nabla_{q_u} M^{-1}(q)p \} + \frac{d}{dt} \{ \nabla_{q_u} V(q) \} \right) \end{aligned}$$

We will compute the explicit expression of  $\ddot{e}$  in pieces to find out where  $\tau$  appears. We begin with  $\frac{d}{dt} \{dh_q\}$ . Let  $h = (h^1, \dots, h^k)$  with  $h^i : \mathcal{Q} \times \mathcal{P}_u \rightarrow \mathbb{R}$ . By definition of the total differential, we have

$$dh_q = \begin{bmatrix} dh_q^1 \\ \vdots \\ dh_q^k \end{bmatrix} = \begin{bmatrix} \frac{\partial h^1}{\partial q_1} & \cdots & \frac{\partial h^1}{\partial q_n} \\ \vdots & \ddots & \vdots \\ \frac{\partial h^k}{\partial q_1} & \cdots & \frac{\partial h^k}{\partial q_n} \end{bmatrix}$$

The time derivative is taken element-wise, yielding

$$\frac{d}{dt} \{dh_q\} = \begin{bmatrix} \sum_{j=1}^n \frac{\partial^2 h^1}{\partial q_1 \partial q_j} \dot{q}_j & \cdots & \sum_{j=1}^n \frac{\partial^2 h^1}{\partial q_n \partial q_j} \dot{q}_j \\ \vdots & \ddots & \vdots \\ \sum_{j=1}^n \frac{\partial^2 h^k}{\partial q_1 \partial q_j} \dot{q}_j & \cdots & \sum_{j=1}^n \frac{\partial^2 h^k}{\partial q_n \partial q_j} \dot{q}_j \end{bmatrix} + \begin{bmatrix} \sum_{l=1}^{n-k} \frac{\partial^2 h^1}{\partial q_1 \partial p_{u_l}} \dot{p}_{u_l} & \cdots & \sum_{l=1}^{n-k} \frac{\partial^2 h^1}{\partial q_n \partial p_{u_l}} \dot{p}_{u_l} \\ \vdots & \ddots & \vdots \\ \sum_{l=1}^{n-k} \frac{\partial^2 h^k}{\partial q_1 \partial p_{u_l}} \dot{p}_{u_l} & \cdots & \sum_{l=1}^{n-k} \frac{\partial^2 h^k}{\partial q_n \partial p_{u_l}} \dot{p}_{u_l} \end{bmatrix}$$

It is straightforward computation to confirm that each row of this derivative can be written in vector form as follows:

$$\begin{aligned} \frac{d}{dt} \{dh_q^i\} &= \left[ \sum_{j=1}^n \frac{\partial^2 h^i}{\partial q_1 \partial q_j} \dot{q}_j \quad \cdots \quad \sum_{j=1}^n \frac{\partial^2 h^i}{\partial q_n \partial q_j} \dot{q}_j \right] + \left[ \sum_{l=1}^{n-k} \frac{\partial^2 h^i}{\partial q_1 \partial p_{u_l}} \dot{p}_{u_l} \quad \cdots \quad \sum_{l=1}^{n-k} \frac{\partial^2 h^i}{\partial q_n \partial p_{u_l}} \dot{p}_{u_l} \right] \\ &= \dot{q}^\top \text{Hess}_q \{h^i\}^\top + \dot{p}_u^\top \partial_{p_u} \partial_q h^i \\ &= p^\top M^{-1}(q) \text{Hess}_q \{h^i\}^\top - \left( \frac{1}{2} p^\top dM_{q_u}^{-1}(q) (I_{n-k} \otimes p) + dV_{q_u}(q) \right) \partial_{p_u} \partial_q h^i \end{aligned}$$

This means that  $\frac{d}{dt} \{dh_q\}$  is given by

$$\begin{aligned} \frac{d}{dt} \{dh_q\} &= (I_n \otimes (p^\top M^{-1}(q))) \text{Hess}_q \{h\}^\top - \\ &\quad \left( \frac{1}{2} I_n \otimes (p^\top dM_{q_u}^{-1}(q)(I_{n-k} \otimes p)) + I_n \otimes dV_{q_u}(q) \right) \partial_{p_u} \partial_q h \end{aligned} \quad (2.10)$$

For the next segment, let  $1_j \in \mathbb{R}^n$  be the vector of all zeros, except for a single 1 at position  $j$ . We define  $C_1 : \mathcal{Q} \times \mathcal{P} \rightarrow \mathbb{R}^{n \times n}$  by

$$C_1(q, p) := \sum_{j=1}^n \frac{\partial M^{-1}}{\partial q_j}(q) \dot{q}_j = \sum_{j=1}^n \frac{\partial M^{-1}}{\partial q_j}(q) (1_j^\top M^{-1}(q) p) \quad (2.11)$$

Moving on to  $\frac{d}{dt} \{dh_{p_u}\}$ , a similar approach to  $\frac{d}{dt} \{dh_q\}$  yields the derivative in matrix form. It is given by:

$$\begin{aligned} \frac{d}{dt} \{dh_{p_u}\} &= (I_n \otimes (p^\top M^{-1}(q))) \partial_q \partial_{p_u} h - \\ &\quad \left( \frac{1}{2} I_n \otimes ((I_{n-k} \otimes p^\top) \nabla_{q_u} M^{-1}(q) p) + I_n \otimes \nabla_{q_u} V(q) \right) \text{Hess}_{p_u} \{h\}^\top \end{aligned} \quad (2.12)$$

For the next piece, observe that the  $i^{\text{th}}$  row of  $\frac{1}{2} \frac{d}{dt} \{ (I_{n-k} \otimes p^\top) \nabla_{q_u} M^{-1}(q) p \}$  is given by

$$\frac{1}{2} \frac{d}{dt} \left\{ p^\top \frac{\partial M^{-1}}{\partial q_{u_i}}(q) p \right\} = p^\top \frac{\partial M^{-1}}{\partial q_{u_i}}(q) \dot{p} + \frac{1}{2} p^\top \left( \sum_{j=1}^n \frac{\partial^2 M^{-1}}{\partial q_{u_i} \partial q_j} \dot{q}_j \right) p$$

Defining  $C_2 : \mathcal{Q} \times \mathcal{P} \rightarrow \mathbb{R}^{n(n-k) \times n}$  by

$$C_2(q, p) := \begin{bmatrix} \sum_{j=1}^n \frac{\partial^2 M^{-1}}{\partial q_{u_1} \partial q_j} (1_j^\top M^{-1}(q) p) \\ \vdots \\ \sum_{j=1}^n \frac{\partial^2 M^{-1}}{\partial q_{u_{n-k}} \partial q_j} (1_j^\top M^{-1}(q) p) \end{bmatrix} \quad (2.13)$$

allows us to collapse the derivative into:

$$\begin{aligned} \frac{1}{2} \frac{d}{dt} \{ (I_{n-k} \otimes p^\top) \nabla_{q_u} M^{-1}(q) p \} &= \\ (I_{n-k} \otimes p^\top) \nabla_{q_u} M^{-1}(q) \left( -\frac{1}{2} (I_{n-k} \otimes p^\top) \nabla_{q_u} M^{-1}(q) p - \nabla_{q_u} V(q) + \begin{bmatrix} \mathbf{0}_{(n-k) \times k} \\ I_k \end{bmatrix} \tau \right) &+ \\ \frac{1}{2} (I_{n-k} \otimes p^\top) C_2(q, p) p & \end{aligned} \quad (2.14)$$

Finally, we compute the derivative of  $\nabla_{q_u} V(q)$ :

$$\frac{d}{dt} \{ \nabla_{q_u} V(q) \} = \begin{bmatrix} \sum_{j=1}^n \frac{\partial^2 V}{\partial q_{u_1} \partial q_j} \dot{q}_j \\ \vdots \\ \sum_{j=1}^n \frac{\partial^2 V}{\partial q_{u_{n-k}} \partial q_j} \dot{q}_j \end{bmatrix} = \partial_{q_u} \partial_q V(q) \dot{q} = \partial_{q_u} \partial_q V(q) M^{-1}(q) p \quad (2.15)$$

Putting this all together, we can find the explicit form for  $\ddot{e}$ :

$$\begin{aligned} \ddot{e} = & \frac{d}{dt} \{ dh_q \} M^{-1}(q) p + dh_q C_1(q, p) p - \\ & \frac{1}{2} dh_q M^{-1}(q) ((I_n \otimes p^\top) \nabla_q M^{-1}(q) p) + dh_q M^{-1}(q) \nabla_q V(q) - \\ & \frac{d}{dt} \{ dh_{p_u} \} \left( \frac{1}{2} (I_{n-k} \otimes p^\top) \nabla_{q_u} M^{-1}(q) p + \nabla_{q_u} V(q) \right) + \\ & dh_{p_u} (I_{n-k} \otimes p^\top) \nabla_{q_u} M^{-1}(q) \left( \frac{1}{2} (I_{n-k} \otimes p^\top) \nabla_{q_u} M^{-1}(q) p + \nabla_{q_u} V(q) \right) - \\ & \frac{1}{2} dh_{p_u} (I_{n-k} \otimes p^\top) C_2(q, p) p - dh_{p_u} \partial_{q_u} \partial_q V(q) M^{-1}(q) p + \\ & (dh_q M^{-1}(q) - dh_{p_u} (I_{n-k} \otimes p^\top) \nabla_{q_u} M^{-1}(q)) \begin{bmatrix} \mathbf{0}_{(n-k) \times k} \\ I_k \end{bmatrix} \tau \end{aligned} \quad (2.16)$$

For shorthand, we'll write  $\ddot{e} = E(q, p) + H(q, p) \tau$  where  $E$  and  $H$  are defined appropriately. From the definition of regularity, the VNHC  $h$  is regular when  $e$  is of relative degree  $\{2, \dots, 2\}$ , which is true if and only if one can solve for  $\tau$  when  $\ddot{e} = 0$ . This is equivalent to requiring that the matrix  $H$  be invertible, proving the theorem.  $\square$

Using the expression  $\ddot{e} = E(q, p) + H(q, p) \tau$  from the proof of Theorem 2, a regular VNHC of order  $k$  can be stabilized by the output-linearizing phase-feedback controller (2.17).

$$\tau(q, p) = -H^{-1}(q, p) (E(q, p) + k_p e + k_d \dot{e}) \quad (2.17)$$

where  $k_p, k_d \in \mathbb{R}_{>0}$  are control parameters which can be tuned on the resulting linear system  $\ddot{e} = -k_p e - k_d \dot{e}$ .

Note that one generally cannot measure conjugate of momenta directly, as sensors on mechanical systems will only measure the state  $(q, \dot{q})$ . To implement this controller in practice, one must compute  $p = M(q) \dot{q}$  at every iteration. In other words, this controller requires knowledge of the full state of the system.

Now that we have found a controller to enforce a regular VNHC of order  $k$ , we would like to solve for the closed-loop dynamics. Intuitively, these dynamics should be parameterized by  $(q_u, p_u)$  since  $q_a$  is a function of these as specified by  $h(q, p_u) = 0$ .

Unfortunately,  $\dot{q}_u$  depends on  $p_a$ , and for general systems one cannot solve explicitly for  $p_a$  in terms of  $(q_u, p_u)$ . This is because the  $\dot{p}$  dynamics contains the coupling term  $(I_n \otimes p^\top) \nabla_{q_u} M(q)p$ .

We now introduce a class of systems where explicitly solving for the closed-loop dynamics is feasible.

**Definition 5.** A mechanical system is **TODO: name this** — if  $\nabla_{q_u} M(q) = \mathbf{0}_{n(n-k) \times n}$ .

**Theorem 3.** Let  $\mathcal{H}$  be a — mechanical system satisfying Assumption 4. Let  $h(q, p_u) = 0$  be a regular VNHC of order  $k$  with constraint manifold  $\Gamma$ . Suppose that on  $\Gamma$  one can solve linearly for  $q_a$  as a function of  $(q_u, p_u)$ . Then the closed-loop dynamics are given by

$$\begin{aligned} \dot{q}_u &= \begin{bmatrix} I_{(n-k)} & \mathbf{0}_{(n-k) \times k} \end{bmatrix} M^{-1}(q)p \\ \dot{p}_u &= -\nabla_{q_u} V(q) \end{aligned} \quad \left| \begin{array}{l} h(q, p_u) = 0 \\ p_a = g(q_u, p_u) \end{array} \right. \quad (2.18)$$

where

$$\begin{aligned} g(q, p_u) &:= \\ &\left( dh_q M^{-1}(q) \begin{bmatrix} \mathbf{0}_{(n-k) \times k} \\ I_k \end{bmatrix} \right)^{-1} \left( dh_{p_u} \nabla_{q_u} V(q) - dh_q M^{-1}(q) \begin{bmatrix} I_{n-k} \\ \mathbf{0}_{k \times (n-k)} \end{bmatrix} p_u \right) \Big|_{h(q, p_u)=0} \end{aligned} \quad (2.19)$$

*Proof.* Setting  $e = h(q, p_u)$  and using the fact that  $\nabla_{q_u} M^{-1}(q) = 0$ , we find that

$$\dot{e} = dh_q M^{-1}(q)p - dh_{p_u} \nabla_{q_u} V(q)$$

Observe that

$$\begin{aligned} dh_q M^{-1}(q)p &= dh_q M^{-1}(q) \begin{bmatrix} p_u \\ p_a \end{bmatrix} \\ &= dh_q M^{-1}(q) \begin{bmatrix} I_{n-k} & \mathbf{0}_{(n-k) \times k} \\ \mathbf{0}_{k \times (n-k)} & I_k \end{bmatrix} \begin{bmatrix} p_u \\ p_a \end{bmatrix} \\ &= dh_q M^{-1}(q) \begin{bmatrix} I_{n-k} \\ \mathbf{0}_{k \times (n-k)} \end{bmatrix} p_u + dh_q M^{-1}(q) \begin{bmatrix} \mathbf{0}_{(n-k) \times k} \\ I_k \end{bmatrix} p_a \end{aligned}$$

On the constraint manifold, we have  $e = \dot{e} = 0$ , which means

$$dh_q M^{-1}(q) \begin{bmatrix} \mathbf{0}_{(n-k) \times k} \\ I_k \end{bmatrix} p_a = dh_{p_u} \nabla_{q_u} V(q) - dh_q M^{-1}(q) \begin{bmatrix} I_{n-k} \\ \mathbf{0}_{k \times (n-k)} \end{bmatrix} p_u$$

Since  $h$  is regular and  $\nabla_{q_u} M^{-1}(q) = 0$ , we have that

$$\text{rank} \left( dh_q M^{-1}(q) \begin{bmatrix} \mathbf{0}_{(n-k) \times k} \\ I_k \end{bmatrix} \right) = k$$

Solving for  $p_a$  gives

$$p_a(q, p_u) = \left( dh_q M^{-1}(q) \begin{bmatrix} \mathbf{0}_{(n-k) \times k} \\ I_k \end{bmatrix} \right)^{-1} \left( dh_{p_u} \nabla_{q_u} V(q) - dh_q M^{-1}(q) \begin{bmatrix} I_{n-k} \\ \mathbf{0}_{k \times (n-k)} \end{bmatrix} p_u \right)$$

This yields a function  $p_a(q, p_u)$ . However, on  $\Gamma$  we have  $h(q, p_u) = 0$  and can solve for  $q_a$  in terms of  $(q_u, p_u)$ ; hence, we can solve for  $p_a = g(q_u, p_u)$ . Since  $q_a$  and  $p_a$  can be computed directly from  $(q_u, p_u)$ , the dynamics on  $\Gamma$  are parameterized only by  $(\dot{q}_u, \dot{p}_u)$ .

**MANFREDI: Do we need this assumption that  $q_a$  can be solved in terms of  $(q_u, p_u)$  or is there some other way of parameterizing it like you did with  $s$  for VHCs?**  $\square$

Theorem 3 shows that, for a particular class of systems and constraints, the dynamics on  $\Gamma$  are entirely described by the  $2(n-k)$  unactuated coordinates. This is true regardless of the number of degrees of freedom of the system, which means that  $\Gamma$  is a  $2(n-k)$ -dimensional surface inside  $\mathcal{Q} \times \mathcal{P}$ .

The following corollary applies Theorem 3 to systems with only one unactuated coordinate.

**Corollary.** *Suppose  $\mathcal{H}$  is a — mechanical system satisfying Assumption 4 which has degree of underactuation one. Let  $h(q, p_u) = 0$  be a regular VNHC of order  $(n-1)$  of the form  $h(q, p_u) = q_a - f(q_u, p_u)$  where  $f$  is a suitably-defined smooth function. Then  $dh_q = [-\partial f_{q_u} \quad I_{(n-1)}]$ . Defining  $e_1 := (1, 0, \dots, 0) \in \mathbb{R}^n$ , the actuated momentum is given by (2.20):*

$$p_a = - \left( dh_q M^{-1}(q) \begin{bmatrix} \mathbf{0}_{1 \times (n-1)} \\ I_{(n-1)} \end{bmatrix} \right)^{-1} \left( \partial_{p_u} f \partial_{q_u} V + dh_q M^{-1}(q) e_1 p_u \right) \Big|_{q_a = f(q_u, p_u)} \quad (2.20)$$

Since  $q_u \in [\mathbb{R}]_T$  for some  $T \in ]0, \infty]$  and  $p_u \in \mathbb{R}$ , the orbit  $(q_u(t), p_u(t))$  traces out a curve on the 2D-plane  $[\mathbb{R}]_T \times \mathbb{R}$  which we call the  $(q, p)$ -plane.

## 2.4 Summary of Results

**TODO: summarize the assumptions and results**



## Chapter 3

# Application of VNHCS: The Variable Length Pendulum

### 3.1 Motivation

The variable length pendulum (VLP) is a classical underactuated dynamical system which is often used to model the motion of a person on a swing [8, 16]. The VLP also represents the motion of the load at the end of a crane, the (simplified) motion of a gymnast on a bar [15], and the tuned-mass-damper systems which stabilize skyscrapers [41].

The motion of the VLP has been well studied (see for instance [39]), and many control mechanisms exist to stabilize trajectories of the system. While many of these controllers are time-dependent, Xin and Liu [20] offer a time-independent technique to inject energy into the system. They designed a controller through a technique called *energy shaping*, and proved that their control mechanism would allow the VLP to achieve any desired energy level set. However, the energy injection mechanism is ad-hoc in the sense that it is not derived from natural behaviour. In this chapter we will design VNHCS to inject energy into the VLP in a time-independent way. The difference compared to [20] is that our controller will maintain the structured motion of a human on a swing.

### 3.2 Dynamics of the Variable Length Pendulum

We will model the VLP as a point mass  $m$  connected to a fixed pivot by a massless rod of varying length  $l$  with angle  $q \in \mathbb{S}^1$  from the vertical, as is seen in Figure 3.1. We will also ignore any damping and frictional forces in this model. In a realistic VLP, the rod

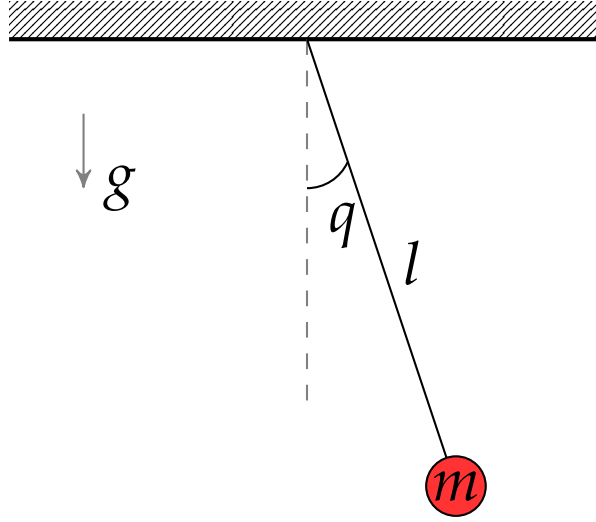


FIGURE 3.1: The representation of the variable length pendulum as a mass at the tip of a massless rod.

length  $l$  varies between some minimum length  $\underline{l} \geq 0$  and some maximum length  $\bar{l} > \underline{l}$ . The configuration of the VLP is the vector  $\mathbf{q} := (q, l) \in \mathbb{S}^1 \times [\underline{l}, \bar{l}]$ .

Using this configuration, we will compute the Hamiltonian dynamics of the system. The cartesian position of the mass at the tip of the pendulum is given by  $x = (l \sin(q), l \cos(q))$ , while its velocity is  $\dot{x} = (\dot{l} \sin(q) + l \cos(q) \dot{q}, \dot{l} \cos(q) - l \sin(q) \dot{q})$ . Computing the kinetic energy  $T$  yields

$$T(\mathbf{q}, \dot{\mathbf{q}}) = \frac{1}{2} m \|\dot{x}\|^2 = \frac{1}{2} m (\dot{l}^2 + l^2 \dot{q}^2)$$

The potential energy  $P$  with respect to the pivot (under a gravitational acceleration  $g$ ) is

$$P(\mathbf{q}) = -mgl \cos(q)$$

Collecting the kinetic energy into a quadratic form, we get the Lagrangian

$$\mathcal{L}(\mathbf{q}, \dot{\mathbf{q}}) = \frac{1}{2} \dot{\mathbf{q}}^T D(\mathbf{q}) \dot{\mathbf{q}} - P(\mathbf{q}) = \frac{1}{2} \begin{bmatrix} \dot{q} & \dot{l} \end{bmatrix} \begin{bmatrix} ml^2 & 0 \\ 0 & m \end{bmatrix} \begin{bmatrix} \dot{q} \\ \dot{l} \end{bmatrix} + mgl \cos(q)$$

Computing the conjugate of momenta to  $\mathbf{q}$ , we get

$$\mathbf{p} := \begin{bmatrix} p \\ p_l \end{bmatrix} = \begin{bmatrix} ml^2 \dot{q} \\ m \dot{l} \end{bmatrix}$$

Performing the Legendre transform on  $\mathcal{L}$  and setting  $M(\mathbf{q}) := D(\mathbf{q})$ ,  $V(\mathbf{q}) := P(\mathbf{q})$ , we

find the Hamiltonian is equal to the total mechanical energy of the system:

$$\mathcal{H} = E = \frac{1}{2} \dot{\mathbf{p}}^\top M^{-1}(\mathbf{q}) \dot{\mathbf{p}} + V(\mathbf{q})$$

Taking the appropriate derivatives, the dynamics of the VLP in Hamiltonian form are described in (3.1).

$$\begin{aligned} \mathcal{H} &= \frac{1}{2} \begin{bmatrix} p & p_l \end{bmatrix} \begin{bmatrix} \frac{1}{ml^2} & 0 \\ 0 & \frac{1}{m} \end{bmatrix} \begin{bmatrix} p \\ p_l \end{bmatrix} - mgl \cos(q) \\ \begin{cases} \dot{q} &= \frac{p}{ml^2} \\ \dot{l} &= \frac{p_l}{m} \\ \dot{p} &= -mgl \sin(q) \\ \dot{p}_l &= \frac{p^2}{ml^3} + mg \cos(q) + \tau \end{cases} \end{aligned} \quad (3.1)$$

The control input is a force  $\tau \in \mathbb{R}$  affecting the dynamics of  $p_l$ , acting colinearly with direction of the rod. We assume the force does not affect the dynamics of  $p$  in any way - that is, the control input cannot enact any lateral force on the pendulum. This is extremely useful for simplifying the dynamics: since one can choose  $\tau$  which sets  $\dot{p}_l$  to any desired function, we can assume (with abuse of notation) that  $l$  is tracking some known function  $l(t)$ . The closed loop dynamics of the system will be described exclusively by  $(q, \dot{p})$  with  $l \equiv l(t)$ . The fact that  $p_l$  does not appear in these closed-loop dynamics allows us to ignore the subdynamics  $(\dot{l}, \dot{p}_l)$  entirely.

What this means is we can treat  $l$  as the control input directly, rather than modelling it as a configuration variable. Re-deriving the Hamiltonian and the dynamics from this approach, we get the system (3.2) with phase  $(q, p) \in \mathbb{S}^1 \times \mathbb{R}$ . Note that the control input  $l(t)$  and its derivative  $\dot{l}(t)$  are both known variables.

$$\begin{aligned} \mathcal{H}(q, p) &= \frac{p^2}{ml^2} - \frac{1}{2} \dot{l}^2 - mgl \cos(q) \\ \begin{cases} \dot{q} &= \frac{p}{ml^2} \\ \dot{p} &= -mgl \sin(q) \end{cases} \end{aligned} \quad (3.2)$$

In particular, the Hamiltonian of this simplified model is no longer equal to the total mechanical energy of the system, which is given by (3.3).

$$E(q, p) = \frac{p^2}{ml^2} + \frac{1}{2} \dot{l}^2 - mgl \cos(q) \quad (3.3)$$



(A) A person standing on a swing has their center of mass close to the pivot.

(B) When a person squats on a swing, their center of mass extends away from the pivot.

FIGURE 3.2: The variable length pendulum representation of a person on a standing swing.

### 3.3 The VLP Constraint

Since we wish to define a VNHCS which injects energy into the VLP in a human-like manner, we return once again to the example of a person standing on a swing. As can be seen in Figure 3.2, condensing the person into a center of mass gives a VLP model of their motion, where the pendulum shrinks when the person stands and lengthens when they squat. This is equivalent to the VLP model from Figure 3.1.

The action of regulating pendulum length to add energy to the VLP is known as “pumping”. Piccoli and Kulkarni asked whether the pumping strategy performed by children is time-optimal, assuming the children could squat or stand instantaneously [16]. Indeed, they discovered that a child’s pumping strategy will inject energy into the VLP as fast as is physically possible.

This pumping strategy is straightforward: the child stands up at the lowest point of their swing, and squats at the highest point. Looking at their VLP representation, the pendulum shortens at the bottom of the swing, and lengthens at the top. For an intuitive understanding, conservation of angular momentum indicates that shortening the pendulum at the bottom forces the mass to gain speed to compensate for the reduced length [8]. Energy is not conserved in this process, and the pendulum gains kinetic energy which allows the pendulum to reach a higher point in its swing. Lengthening the

pendulum when it reaches this point means gravity imparts a larger angular momentum to the mass by the time it reaches the bottom of its swing, which is converted into a higher velocity the next time the pendulum is shortened. By alternating these processes, the pendulum experiences a net gain in rotational energy which is generated entirely by gravity.

The time-optimal controller described by [16] depends on a trajectory in time. We will convert this into a time-independent controller derived from the time-optimal strategy. Notice that the optimal controller depends on knowing when the system is at the “bottom” or “top” of the swing. Since being at the “bottom” is the same as saying the pendulum angle is  $q = 0$  and being at the “top” is equivalent to the pendulum’s momentum being  $p = 0$ , the time-independent controller will necessarily use the full phase  $(q, p)$ . While VHCs cannot satisfy this requirement, our method of VNHCS is especially well suited to this problem.

Figure 3.3a shows the time-optimal strategy directly on the  $(q, p)$ -plane. Since the VLP must stay the same length inside each quadrant and changes length only when it crosses one of the axes, we will use the angle  $\theta = \arctan_2(p, q)$  in the  $(q, p)$ -plane to define the optimal controller  $l^*(\theta)$  (3.4). Figure 3.3b shows this time-optimal controller as a function of  $\theta$ .

$$l^*(\theta) := \begin{cases} \underline{l} & \theta \in [-\pi, -\frac{\pi}{2}] \cup [0, \frac{\pi}{2}] \\ \bar{l} & \theta \in [-\frac{\pi}{2}, 0] \cup [\frac{\pi}{2}, \pi] \end{cases} \quad (3.4)$$

To find a continuously differentiable function which approximates this controller, we can attach sinusoids at the transition points of  $l^*(\theta)$  (see Figure 3.4). Let  $\Delta l := (\bar{l} - \underline{l})/2$  and  $l_{\text{avg}} := (\bar{l} + \underline{l})/2$ . Providing these newly attached sinusoids with a frequency  $\omega = \frac{2\pi}{T}$  (where  $T \in ]0, \frac{\pi}{2}]$  is a control parameter), we have a new controller  $l_T(\theta)$ :

$$l_T(\theta) = \begin{cases} \underline{l} & \theta \in \left[-\pi + \frac{T}{2}, -\frac{\pi}{2} - \frac{T}{2}\right] \cup \left[\frac{T}{2}, \frac{\pi}{2} - \frac{T}{2}\right] \\ \bar{l} & \theta \in \left[-\frac{\pi}{2} + \frac{T}{2}, -\frac{T}{2}\right] \cup \left[\frac{\pi}{2} + \frac{T}{2}, \pi - \frac{T}{2}\right] \\ -\Delta l \sin(\omega(\theta + \pi)) + l_{\text{avg}} & \theta \in \left[-\pi, -\pi + \frac{T}{2}\right] \\ -\Delta l \sin(\omega\theta) + l_{\text{avg}} & \theta \in \left[-\frac{T}{2}, \frac{T}{2}\right] \\ \Delta l \sin(\omega(\theta - a)) + l_{\text{avg}} & \theta \in \left[a - \frac{T}{2}, a + \frac{T}{2}\right] \text{ for } a \in \left\{-\frac{\pi}{2}, \frac{\pi}{2}\right\} \\ -\Delta l \sin(\omega(\theta - \pi)) & \theta \in \left[\pi - \frac{T}{2}, \pi\right] \end{cases} \quad (3.5)$$

This controller approximates the optimal controller, since

$$\lim_{T \rightarrow 0} l_T(\theta) = l^*(\theta)$$

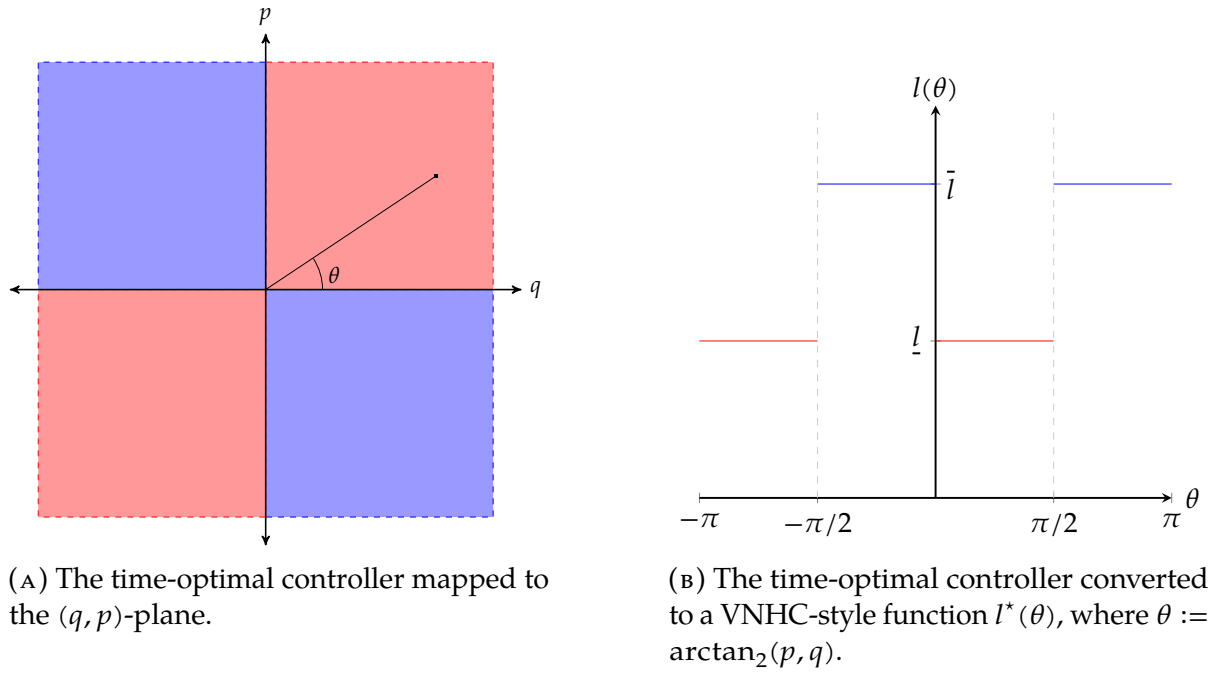


FIGURE 3.3: The time-optimal controller for a standing swing as derived by [16]. The colour red corresponds to standing and blue to squatting.

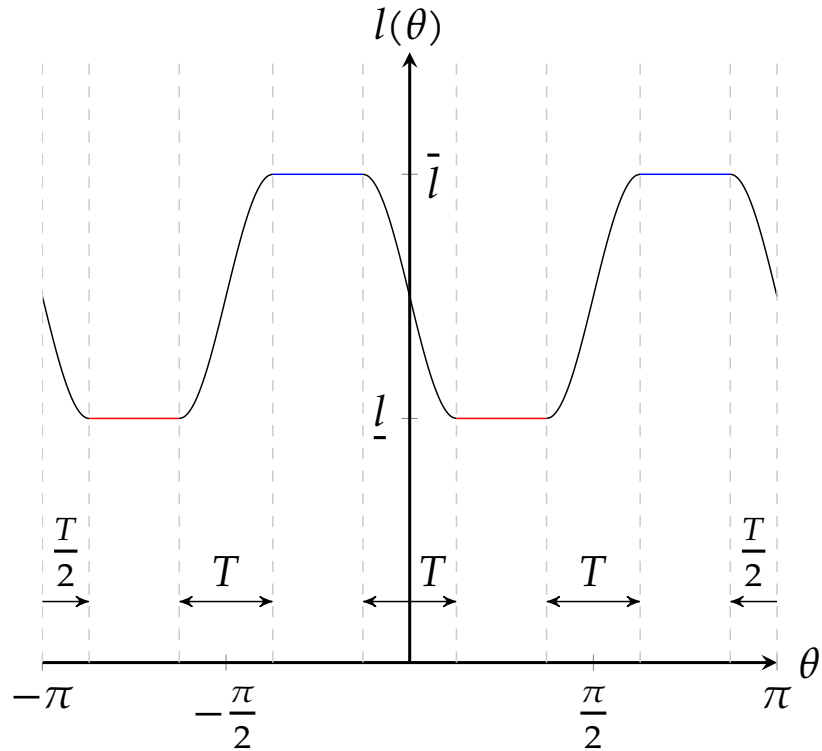


FIGURE 3.4: The continuous VNHC-style VLP controller  $l_T(\theta)$ .

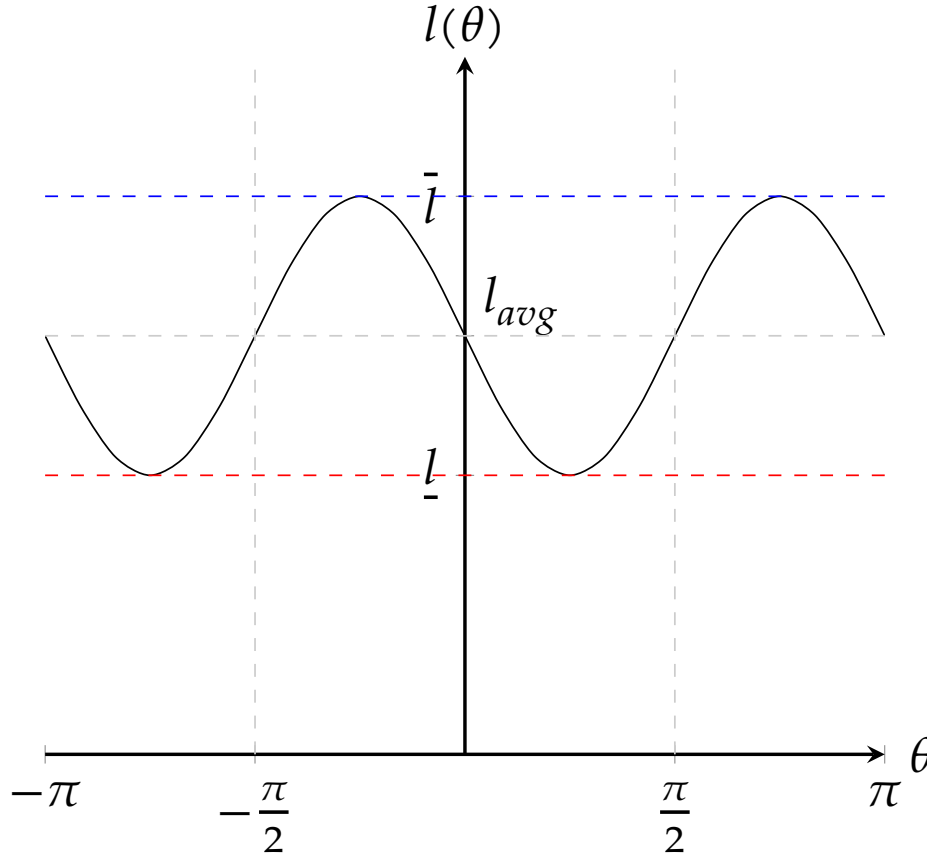


FIGURE 3.5: The smoothed VLP controller which corresponds to the VNHC  $l = l_{\frac{\pi}{2}}(\theta)$ .

Unfortunately, while  $l_T(\theta)$  is continuously differentiable, it is not twice continuously differentiable for most values of  $T$ . If we wish to use it as a VNHC, we must ensure that either the generalized forces  $\tau$  acting on  $p_l$  can be discontinuous, or we must find a value of  $T$  where this controller is smooth. Thankfully,  $l_{\frac{\pi}{2}}(\theta)$  is smooth; it can be simplified into the expression (3.6), and is plotted for demonstration in Figure 3.5.

$$l_{\frac{\pi}{2}}(\theta) = -\Delta l \sin(2\theta) + l_{\text{avg}} \quad (3.6)$$

We therefore set our VNHC to be

$$h(q, p) = l - l_{\frac{\pi}{2}}(\theta(q, p))$$

This VNHC is not the same as the optimal controller (3.4), so we need to prove it will still gain energy. We will do so by showing the dynamics (3.2) of the VLP diverge from the origin, regardless of the initial condition of the system. To do this, we will use the notion of an anti-Lyapunov function.

**Definition 6.** Let  $\dot{x} = f(x) \in \mathbb{R}^n$  be an ODE with  $f(0) = 0$ . A positive definite function  $V(x)$  is **anti-Lyapunov** if

$$\dot{V}(x) = dV(x)f(x) \geq 0$$

where the inequality is strict for almost every  $x \in \mathbb{R}^n$ .

By applying Lyapunov stability theory [42], we see that an anti-Lyapunov function  $V$  is simply a Lyapunov function for the negative-time system  $\dot{x} = -f(x)$ . In other words, since  $V$  proves that the orbit  $x(-t)$  of the system travelling backwards in time is asymptotically converging to the equilibrium, the system must be diverging from the equilibrium in forward time. If we can find such a function for the VLP's dynamics under our VNHC, the path generated by the VNHC in the  $(q, p)$ -plane must be diverging from the origin so long as the initial condition is not an equilibrium. This in turn tells us the magnitude of the momentum  $p$  is increasing every time the path hits the  $p$ -axis, which means the VLP is, on average, increasing in energy.

We will show that anti-Lyapunov function exists for our VNHC. In order to do so, we require the following lemma.

**Lemma 1.** For any  $x, y \in \mathbb{R}$ :

$$\text{sgn}(x^3 - y^3) = \text{sgn}(x - y)$$

*Proof.* Observe first that

$$x^3 - y^3 = (x - y)(x^2 + xy + y^2)$$

Since  $(x - y)^2 = x^2 - 2xy + y^2 \geq 0$ ,

$$\frac{x^2 + y^2}{2} \geq xy$$

which means  $x^2 + xy + y^2 \geq 0$ , proving the lemma.  $\square$

**Theorem 4.** Take the VLP with Hamiltonian dynamics (3.2) and define  $\theta := \arctan_2(p, q)$ . Suppose the initial condition is not one of the equilibria:  $(q(0), p(0)) \notin \{(0, 0), (\pm\pi, 0)\}$ . A VNHC of the form  $h(q, p) = l - l(\theta)$  injects energy if there exists  $l_{\text{avg}} \in [l, \bar{l}]$  such that

$$(l(\theta) - l_{\text{avg}}) \sin(2\theta) \leq 0 \quad \forall \theta \in \mathbb{S}^1 \quad (3.7)$$

with the property that the inequality is strict for almost every  $\theta$ . Flipping the inequality of (3.7) leads to energy dissipation.



*Proof.* Choose, as a candidate anti-Lyapunov function, the energy for the average-length pendulum (with zero potential at the bottom of the swing)

$$E_{\text{avg}}(q, p) := \frac{1}{2} \frac{p^2}{ml_{\text{avg}}^2} + mgl_{\text{avg}}(1 - \cos(q))$$

which is positive definite at  $(0, 0)$  and has derivative

$$\dot{E}_{\text{avg}} = \frac{-g \sin(q)p (l(\theta)^3 - l_{\text{avg}}^3)}{l_{\text{avg}}^2 l(\theta)^2}$$

Observe that  $\text{sgn}(\sin(q)p) = \text{sgn}(\sin(2\theta))$  and, by Lemma 1,

$$\text{sgn}(l(\theta)^3 - l_{\text{avg}}^3) = \text{sgn}(l(\theta) - l_{\text{avg}})$$

Then the derivative of  $E_{\text{avg}}$  is almost always positive, since

$$\begin{aligned} \text{sgn}(\dot{E}_{\text{avg}}) &= \text{sgn}(-\sin(q)p (l(\theta)^3 - l_{\text{avg}}^3)) \\ &= -\text{sgn}(\sin(2\theta) (l(\theta) - l_{\text{avg}})) \\ &\geq 0 \text{ (by assumption)} \end{aligned}$$

Hence,  $E_{\text{avg}}$  is an anti-Lyapunov function. Since the initial condition is not an equilibrium, the orbit of the VNHC in the  $(q, p)$  plane is diverging away from the origin and the VLP is gaining energy on average. Flipping the inequality of (3.7) means  $E_{\text{avg}}$  is a regular Lyapunov function, since its derivative will be negative almost everywhere.  $\square$

**Corollary.** *The VNHC  $l = l_{\frac{\pi}{2}}(\theta)$  injects energy into the VLP over time, since*

$$(l_{\frac{\pi}{2}}(\theta) - l_{\text{avg}}) \sin(2\theta) = -\Delta l \sin^2(2\theta) \geq 0$$

*Likewise, let  $l_{\frac{\pi}{2}}^{-1}(\theta) := l_{\text{avg}} - \Delta l \sin(2\theta)$ . The VNHC  $h(q, p) = l - l_{\frac{\pi}{2}}^{-1}(\theta)$  which flips  $l_{\frac{\pi}{2}}(\theta)$  about  $l_{\text{avg}}$  will dissipate energy from the VLP, since*

$$(l_{\frac{\pi}{2}}^{-1}(\theta) - l_{\text{avg}}) \sin(2\theta) = -\Delta l \sin^2(2\theta) \leq 0$$

The types of VNHCS which satisfy Theorem 4 are illustrated by Figure 3.6. To stabilize specific energy level sets, one simple approach is to switch between injection and dissipation VNHCS depending on the current energy level. For the VNHCS we

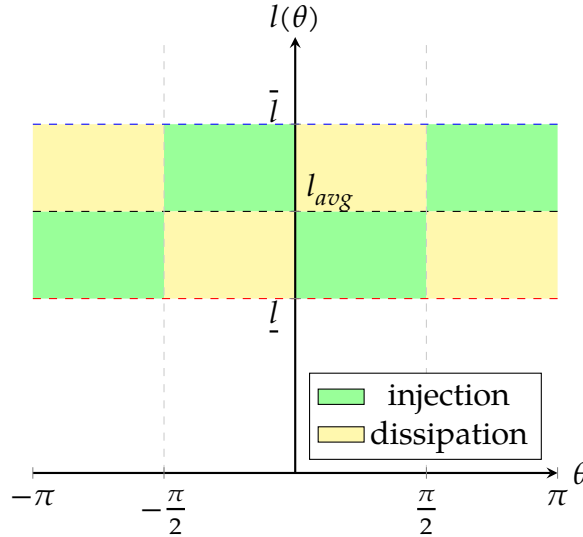


FIGURE 3.6: A VNHC of the form  $l(\theta)$  which is entirely contained within the green (yellow) regions will inject (dissipate) energy into the VLP because it will satisfy Theorem 4.

designed in this section, this means toggling between  $l_{\frac{\pi}{2}}(\theta)$  and  $l_{\frac{\pi}{2}}^{-1}(\theta)$ , possibly with some hysteresis to avoid infinite switching.

Theorem 4 also provides an alternate explanation for why the “optimal” VNHC  $l^*(\theta)$  works so well at injecting energy: it maximizes the derivative of  $E_{\text{avg}}$  under the restriction  $l(\theta) \in [l, \bar{l}]$ , so that the orbit in the  $(q, p)$ -plane diverges from the origin as fast as possible.

Let us define  $(l^*)^{-1}(\theta)$  by swapping the order of  $l$  and  $\bar{l}$  in  $l^*(\theta)$ . Since this *minimizes* the derivative of  $E_{\text{avg}}$  under the restriction  $l(\theta) \in [l, \bar{l}]$ , we can predict that  $(l^*)^{-1}(\theta)$  is the VNHC representation of an optimal energy dissipation controller. This is, in fact, true: [16] showed that squatting at the lowest point of a swing and standing at the highest point (instead of standing and squatting resp.) produces the time-optimal trajectory for stopping a standing swing.

All together, these results show that VNHCS can replicate the time-optimal strategy performed by humans in a time-independent manner. Furthermore, we see that VNHCS are a powerful tool for creating simple energy stabilization techniques based on natural human motion.

### 3.4 Simulation Results

# Chapter 4

## Application of VNHCs: The Acrobot

### 4.1 Motivation

The acrobot is a two-link pendulum, actuated at the center joint (as in Figure 4.1. Since its first description in 1990 [43], the acrobot has become a benchmark problem in control theory; it is an underactuated mechanical system which produces complex nonlinear motion from an easy-to-describe model. The acrobot models a gymnast on a bar, since it represents a torso (top link) and legs (bottom link) with motion generated by the swinging of the legs at the hips. It is also one of the simplest models for a biped walking robot [44].

Controlling the acrobot is a nontrivial task, since it is not feedback linearizable [43]. Many researchers have studied the swing-up problem of driving the acrobot to its equilibrium point above the bar using partial feedback linearization [45], energy-based control [17, 46], and through studying human motion [18, 47].

In gymnastics terminology, a “giant” is when the gymnast performs full rotations around the bar with their body almost fully extended [48]. We are interested in studying the energy stabilization problem for the acrobot by using VNHCs to generate giant motion. The control of giant motion for the acrobot has been studied thoroughly [2, 5, 18], including several studies which use virtual (holonomic) constraints to achieve this behaviour [2, 3, 21]. However, these controllers are neither intuitive nor easy to design: [2] defines a constraint by inverting a trajectory in time onto the state space; [3] requires a cascade controller to stabilize both a constraint and a desired limit cycle in the state space; and [21] enforces the giant by adding an extra state to estimate the velocity, which increases the dimensionality of the problem as a crude approach to using VNHCs.

In this chapter we will design a physically-intuitive VNHC which generates giant motion. We will prove that this VNHC injects energy into the acrobot; in the process

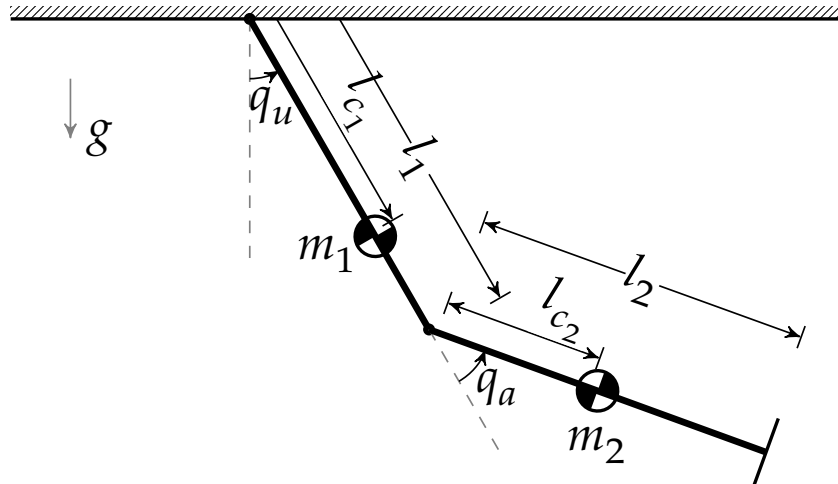
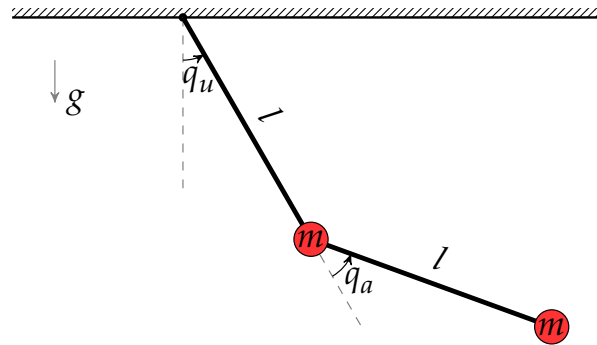


FIGURE 4.1: The acrobot model.

FIGURE 4.2: A simple acrobot with lengths  $l$  and masses of size  $m$ .

of completing this proof, we will describe a promising method which may be used to generate desirable VNHCs in the future.

## 4.2 Dynamics of the Acrobot

For the acrobot model displayed in Figure 4.1, the COM of each link lies somewhere along the link itself. While this is the most general representation of an acrobot, the dynamics are somewhat complicated and are difficult to use when proving the results in the rest of this chapter. For simplicity, we will assume the acrobot is comprised of two massless rods of equal length with equal masses at the tips, as in Figure 4.2; we call this a **simple** acrobot.

### **4.3 Previous Approaches**

### **4.4 The Acrobot Constraint**

### **4.5 Proving the Acrobot Gains Energy**

### **4.6 Experimental Results**

# **Chapter 5**

## **Conclusion**

### **5.1 Limitations of this Work**

### **5.2 Future Research**

# Bibliography

- [1] F. Udwadia, "Constrained motion of hamiltonian systems," *Nonlinear Dynamics*, vol. 84, no. 3, pp. 1135 – 1145, December 2015.
- [2] K. Ono, K. Yamamoto, and A. Imadu, "Control of giant swing motion of a two-link horizontal bar gymnastic robot," *Advanced Robotics*, vol. 15, no. 4, pp. 449 – 465, 2001.
- [3] X. Zhang, H. Cheng, Y. Zhao, and B. Gao, "The dynamical servo control problem for the acrobot based on virtual constraints approach," in *The 2009 IEEE/RSJ International Conference on Intelligent Robots and Systems*. St. Louis, USA: IEEE, October 2009.
- [4] A. Mohammadi, M. Maggiore, and L. Consolini, "Dynamic virtual holonomic constraints for stabilization of closed orbits in underactuated mechanical systems," *Automatica*, vol. 94, pp. 112 – 124, August 2018.
- [5] E. Papadopoulos and G. Papadopoulos, "A novel energy pumping strategy for robotic swinging," in *2009 17th Mediterranean Conference on Control and Automation*. Thessaloniki, Greece: IEEE, June 2009.
- [6] A. J. V. der Schaft, "On the hamiltonian formulation of nonholonomic mechanical systems," *Reports on Mathematical Physics*, vol. 34, no. 2, pp. 225 – 233, 1994.
- [7] O. E. Fernandez, "The hamiltonization of nonholonomic systems and its applications," Ph.D. dissertation, University of Michigan, 2009.
- [8] S. Wirkus, R. Rand, and A. Ruina, "How to pump a swing," *The College Mathematics Journal*, vol. 29, no. 4, pp. 266 – 275, 1998.
- [9] J. Horn, A. Mohammadi, K. Hamed, and R. Gregg, "Hybrid zero dynamics of bipedal robots under nonholonomic virtual constraints," *IEEE Control Systems Letters*, vol. 3, no. 2, pp. 386 – 391, April 2019.

- [10] S. C. Anco and G. Bluman, "Integrating factors and first integrals for ordinary differential equations," *European Journal of Applied Mathematics*, vol. 9, pp. 245 – 259, 1998.
- [11] A. Mohammadi, M. Maggiore, and L. Consolini, "On the lagrangian structure of reduced dynamics under virtual holonomic constraints," *ESAIM: Control, Optimization and Calculus of Variations*, vol. 23, no. 3, pp. 913 – 935, June 2017.
- [12] M. S. Branicky, "Multiple lyapunov functions and other analysis tools for switched and hybrid systems," *IEEE Transactions on Automatic Control*, vol. 43, no. 4, pp. 475 – 482, April 1998.
- [13] J. Lu and L. J. Brown, "A multiple lyapunov functions approach for stability of switched systems," in *2010 American Control Conference*. Baltimore, USA: IEEE, July 2010.
- [14] A. M. Bloch, J. E. Marsden, and D. V. Zenkov, "Nonholonomic dynamics," *Notices of the AMS*, vol. 52, no. 3, pp. 320 – 329, March 2005.
- [15] V. Sevrez, E. Berton, G. Rao, and R. J. Bootsma, "Regulation of pendulum length as a control mechanism in performing the backward giant circle in gymnastics," *Human Movement Science*, vol. 28, no. 2, pp. 250 – 262, March 2009.
- [16] B. Piccoli and J. Kulkarni, "Pumping a swing by standing and squatting: Do children pump time-optimally?" *IEEE Control Systems Magazine*, vol. 25, no. 4, pp. 48 – 56, August 2005.
- [17] A. D. Mahindrakar and R. N. Banavar, "A swing-up of the acrobot based on a simple pendulum strategy," *International Journal of Control*, vol. 78, no. 6, pp. 424 – 429, 2005.
- [18] T. Henmi, M. Chujo, Y. Ohta, and M. Deng, "Reproduction of swing-up and giant swing motion of acrobot based on a technique of the horizontal bar gymnast," in *Proceedings of the 11th World Congress on Intelligent Control and Automation*. Shenyang, China: IEEE, June 2014.
- [19] M. Maggiore and L. Consolini, "Virtual holonomic constraints for euler-lagrange systems," *IEEE Transactions on Automatic Control*, vol. 58, no. 4, pp. 1001 – 1008, April 2013.



- [20] X. Xin and Y. Liu, "Trajectory tracking control of variable length pendulum by partial energy shaping," *Communications in Nonlinear Science and Numerical Simulations*, vol. 19, no. 5, pp. 1544 – 1556, May 2014.
- [21] X. Wang, "Motion control of a gymnastics robot using virtual holonomic constraints," Master's thesis, University of Toronto, 2016.
- [22] H. K. Khalil, *Nonlinear Systems*, 3rd ed. Upper Saddle River, NJ 07485: Prentice Hall, 2002.
- [23] D. T. Greenwood, *Principles of Dynamics*, 2nd ed. Englewood Cliffs, NJ: Prentice Hall, 1987.
- [24] L. D. Landau and E. M. Lifschitz, *Mechanics*, 3rd ed. Butterworth-Heinemann, January 1982.
- [25] J. A. Acosta, R. Ortega, A. Astolfi, and A. Mahindrakar, "Interconnection and damping assignment passivity-based control of mechanical systems with underactuation degree one," *IEEE Transactions on Automatic Control*, vol. 50, no. 12, pp. 1936 – 1955, December 2005.
- [26] A. Mahindrakar, A. Astolfi, R. Ortega, and G. Viola, "Further constructive results on interconnection and damping assignment control of mechanical systems: The acrobot example," in *Proceedings of the 2006 American Control Conference*. Minneapolis, Minnesota, USA: American Control Conference, June 2006.
- [27] J. Grizzle, C. Chevallereau, R. Sinnet, and A. Ames, "Models, feedback control, and open problems of 3d bipedal robotic walking," *Automatica*, vol. 50, no. 8, pp. 1955 – 1988, August 2014.
- [28] F. Plestan, J. Grizzle, E. R. Westervelt, and G. Abba, "Stable walking of a 7-dof biped robot," *IEEE Transactions on Robotics and Automation*, vol. 19, no. 4, pp. 653–668, August 2003.
- [29] A. Mohammadi, E. Rezapour, M. Maggiore, and K. Y. Pettersen, "Maneuvering control of planar snake robots using virtual holonomic constraints," *IEEE Transactions on Control Systems Technology*, vol. 24, no. 3, pp. 884 – 899, May 2015.
- [30] L. Consolini and M. Maggiore, "Control of a bicycle using virtual holonomic constraints," *Automatica*, vol. 49, no. 9, pp. 2831–2839, September 2013.

- [31] S. Westerberg, U. Mettin, A. S. Shiriaev, L. B. Freidovich, and Y. Orlov, "Motion planning and control of a simplified helicopter model based on virtual holonomic constraints," in *2009 International Conference on Advanced Robotics*. Munich, Germany: IEEE, June 2009, pp. 1–6.
- [32] T. Takubo, H. Arai, and K. Tanie, "Virtual nonholonomic constraint for human-robot cooperation in 3-d space," in *2000 IEEE/RSJ International Conference on Intelligent Robots and Systems*. Takamatsu, Japan: IEEE, October 2000.
- [33] S. Shibata and T. Murakami, "Psd based virtual nonholonomic constraint for human interaction of redundant manipulator," in *Proceedings of the 2004 IEEE International Conference on Control Applications*. Taipei, Taiwan: IEEE, September 2004.
- [34] J. D. Castro-Díaz, P. Sánchez-Sánchez, A. Gutiérrez-Giles, M. Arteaga-Pérez, and J. Pliego-Jiménez, "Experimental results for haptic interaction with virtual holonomic and nonholonomic constraints," *IEEE Access*, vol. 8, pp. 120 959 – 120 973, July 2020.
- [35] S. Vozar, Z. Chen, P. Kazanzides, and L. L. Whitcomb, "Preliminary study of virtual nonholonomic constraints for time-delayed teleoperation," in *2015 IEEE/RSJ International Conference on Intelligent Robots and Systems*. Hamburg, Germany: IEEE, October 2015.
- [36] B. Griffin and J. Grizzle, "Nonholonomic virtual constraints for dynamic walking," in *2015 54th IEEE Conference on Decision and Control*. Osaka, Japan: IEEE, December 2015.
- [37] J. C. Horn, A. Mohammadi, K. A. Hamed, and R. D. Gregg, "Nonholonomic virtual constraint design for variable-incline bipedal robotic walking," *IEEE Robotics and Automation Letters*, vol. 5, pp. 3691 – 3698, February 2020.
- [38] W. K. Chan, Y. Gu, and B. Yao, "Optimization of output functions with nonholonomic virtual constraints in underactuated bipedal walking control," in *2018 Annual American Control Conference*. Milwaukee, USA: IEEE, June 2018.
- [39] A. O. Belyakov, A. P. Seyranian, and A. Luongo, "Dynamics of the pendulum with periodically varying length," *Physica D*, vol. 238, pp. 1589 – 1597, August 2009.

- [40] C. Li, Z. Zhang, X. Liu, and Z. Shen, "An improved principle of rapid oscillation suppression of a pendulum by a controllable moving mass: Theory and simulation," *Shock and Vibration*, vol. 2019, April 2019.
- [41] L. Wang, W. Shi, and Y. Zhou, "Study on self-adjustable variable pendulum tuned mass damper," *The structural design of tall and special buildings*, vol. 28, January 2019.
- [42] A. M. Lyapunov, "The general problem of stability of motion (in russian)," Ph.D. dissertation, University of Kharkhov, Kharkhov, Russia, 1892.
- [43] J. Hauser and R. Murray, "Nonlinear controllers for non-integrable systems: the acrobot example," in *1990 American Control Conference*. San Diego, USA: IEEE, May 1990.
- [44] E. Westervelt, "Toward a coherent framework for the control of planar biped locomotion," Ph.D. dissertation, University of Michigan, Michigan, USA, 2003.
- [45] M. W. Spong, "The swing up control problem for the acrobot," *IEEE Control Systems Magazine*, vol. 15, pp. 49–55, February 1995.
- [46] X. Xin and M. Kaneda, "The swing up control for the acrobot based on energy control approach," in *Proceedings of the 41st IEEE Conference on Decision and Control*. Las Vegas, USA: IEEE, March 2003.
- [47] T. Henmi, M. Akiyama, and T. Yamamoto, "Motion control of underactuated linkage robot based on gymnastic skill," *Electrical Engineering in Japan*, vol. 206, pp. 42–50, January 2009.
- [48] P. E. Pidcoe, "The biomechanics principles behind training giant swings," Online, Virginia Commonwealth University, Richmond, VA, USA, August 2005, accessed 11 September 2020. <https://usagym.org/pages/home/publications/technique/2005/8/giant.pdf>.
- [49] G. Golub and W. Kahan, "Calculating the singular values and pseudo-inverse of a matrix," *Journal of the Society for Industrial and Applied Mathematics: Series B, Numerical Analysis*, vol. 2, no. 2, pp. 204–224, 1965.